

Phonon-induced spin squeezing based on geometric phase

Yan-Lei Zhang,^{1,2} Chang-Ling Zou,^{1,2,3,*} Xu-Bo Zou,^{1,2,†} Liang Jiang,³ and Guang-Can Guo^{1,2}

¹Key Laboratory of Quantum Information, University of Science and Technology of China, Hefei, Anhui 230026, China
²Synergetic Innovation Center of Quantum Information & Quantum Physics, University of Science and Technology of China, Hefei, Anhui 230026, China

³Department of Applied Physics, Yale University, New Haven, Connecticut 06511, USA

(Received 15 February 2015; published 14 July 2015)

A scheme to achieve spin squeezing using a geometric phase induced by a single mechanical mode is proposed. The analytical and numerical results show that the ultimate degree of spin squeezing depends on the parameter $\frac{n_{th}+1/2}{Q\sqrt{N}}$, which is the ratio between the thermal excitation, the quality factor, and square root of ensemble size. The undesired coupling between the spin ensemble and the bath can be efficiently suppressed by bang-bang control pulses. With high quality factor, the ultimate limit of the ideal one-axis twisting spin squeezing can be obtained for a nitrogen-vacancy ensemble in diamond.

DOI: [10.1103/PhysRevA.92.013825](https://doi.org/10.1103/PhysRevA.92.013825)

PACS number(s): 42.50.Lc, 42.50.Dv, 03.65.Vf, 85.85.+j

I. INTRODUCTION

The nitrogen-vacancy (NV) centers in diamond are among the most promising implementations of quantum bits for quantum information processing [1] and nanoscale sensors [2], which is because their ground-state spin triplet possesses ultralong coherent time at room temperature [3] and can be read out via optical fluorescence. Significant progress has been achieved in recent experiments to couple the NV electronic spins to nuclear spins [4,5] and mechanical resonators [6,7]. The nanoscale magnetometry [8,9], thermometer [10], and electric field detection [11] have been demonstrated by single NV or an ensemble.

It is well known that the quantum states can boost the precision of measurement beyond the standard quantum limit [12]. Among them, the spin-squeezed states (SSS) [13–16] have attracted much interest and have been applied to spin or atom ensembles for atomic clocks and gravitational wave interferometers. There are many proposals and experiments to realize the spin squeezing in atom ensembles, such as atom-atom collisions [17], quantum nondemolition (QND) measurement [18,19], and cavity squeezing [20–25]. Very recently, spin squeezing of an NV ensemble by Tavis-Cummings type interaction between phonon and spins [26] has been proposed for quantum enhanced magnetometry.

In this paper, we propose an approach for the realization of spin squeezing by phonon-induced geometric phase, using an ensemble of NV centers dispersively coupled to a mechanical resonator. It is shown that the ultimate degree of spin squeezing by one-axis twisting can be realized, for reasonable ratio between the thermal excitation and the quality factor of mechanical oscillators. Furthermore, the effect of the coupling between NV centers and environment is studied, which leads to dephasing and degrades the spin-squeezing effect. By introducing the bang-bang pulse sequence, the decoherence is effectively suppressed and significant spin squeezing can be achieved for the NV ensemble.

II. MODEL

The negatively charged NV center (NV⁻) in diamond is well studied, whose Hamiltonian reads $H_{NV} = (D + d^{\parallel}\epsilon_z)S_z^2 + \mu_B g_e \vec{S} \cdot \vec{B}$ [11,27], where $D \approx 2.87$ GHz is zero-field splitting, d^{\parallel} and ϵ_z are axial ground-state electric dipole moment and electric field (strain field), respectively, μ_B is the Bohr magneton, g_e is the electron g factor, \vec{S} is the electron spin operator, and \vec{B} is the applied magnetic field. With appropriate bias field B_z , the two microwave transitions $|0\rangle \leftrightarrow |\pm 1\rangle$ can be addressed separately in experiment, and we focus on the $\{|0\rangle, |-1\rangle\}$ by applying near-resonant microwaves at the transition $|0\rangle \leftrightarrow |-1\rangle$, which can be treated as a spin- $\frac{1}{2}$ system in the following. The Hamiltonian can be written as $H_{NV-} = (D + d^{\parallel}\epsilon_z - \mu_B g_e B_z)|-1\rangle\langle -1|$, and we have ignored the $|+1\rangle$ state.

Putting the NV⁻ spin ensemble in a gradient magnetic field $\frac{\partial B_z}{\partial u} \neq 0$, then the displacement of diamond or nanomagnet δu will shift the transition frequency by $\Delta\omega_{NV} = -\mu_B g_e \frac{\partial B_z}{\partial u} \delta u$ [28], and the interaction Hamiltonian reads $H_I \propto \sigma_z(a + a^\dagger)$ with $\delta u \propto a + a^\dagger$, where a and a^\dagger are annihilation and creation operators of phonons. Alternatively, the strain field of a diamond nanomechanical oscillator can induce an electric field inside the crystal and give rise to a similar phonon-spin interaction [6,29]. Both approaches to couple the spin with the nanomechanical oscillator have been demonstrated in experiments recently [6,7,28–31]. The simplified Hamiltonian of an ensemble of $2N$ spins coupled to a mechanical resonator is

$$H = \omega_a a^\dagger a + g J_z (a + a^\dagger), \quad (1)$$

where ω_a is the frequency of the mechanical resonator, $J_z = \frac{1}{2} \sum_{j=1}^{2N} \sigma_{zj}$ is the collective spin operator, and g is the single phonon coupling strength. Along with the progress in the nanofabrication of diamond material, various diamond nanomechanical resonators have been realized in experiment, with frequency ranging from 1 kHz to 1 GHz, and the quality factor Q ranging from 100 to around 10^6 [6,29,32–34]. Thus, we study the spin squeezing induced by the mechanical resonator with frequency $\omega_a/2\pi = 1$ MHz and coupling strength $g/2\pi = 1$ KHz [35] in this work.

*clzou321@ustc.edu.cn

†xbz@ustc.edu.cn

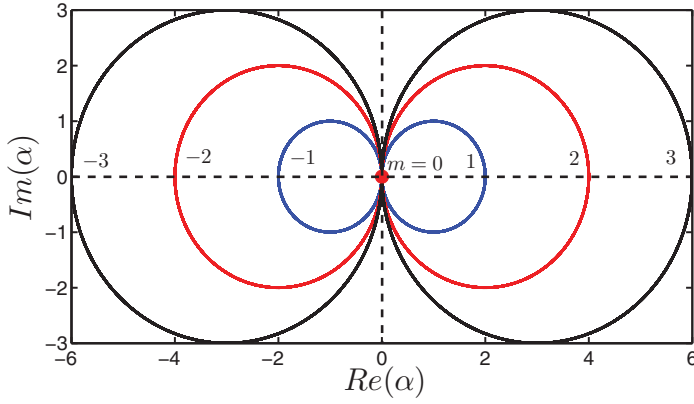


FIG. 1. (Color online) Trajectories on phase space of a coherent wave packet $\langle a \rangle = \text{Re}(\alpha) + i\text{Im}(\alpha)$ for spin state $|m\rangle$ with $m = 0, \pm 1, \pm 2, \pm 3$. Here we set g/ω_a as a unit.

The Hamiltonian preserves J_z of the spin ensemble. The dynamics of the system satisfy the Schrödinger equation $i \frac{\partial |\psi\rangle}{\partial t} = H|\psi\rangle$, and we can obtain the solution $|\psi(t)\rangle = e^{i\phi(t)}|\alpha(t)\rangle$ for an initial coherent state $|\psi(0)\rangle = |\alpha(0)\rangle$, where $\phi(t) = -gJ_z \text{Re} \int_0^t \alpha(\tau) d\tau$ is the geometric phase [36] with $\alpha(t) = \alpha(0)e^{-i\omega_a t} + \frac{-gJ_z}{\omega_a} [1 - e^{-i\omega_a t}]$. It is convenient to study the mechanical resonator by the coherent state $|\alpha\rangle$, and we can write $|\alpha\rangle = |\text{Re}(\alpha) + i\text{Im}(\alpha)\rangle$. The coherent state behaves somehow like classical particles in phase space. Its center, given by $\text{Re}(\alpha)$ and $\text{Im}(\alpha)$, follows a classical trajectory, while the width of these wave packets remains fixed, which is given by the uncertainty of the $\text{Re}(\alpha)$ and $\text{Im}(\alpha)$. In Fig. 1 we plot the usual phase-space trajectories for $\langle a \rangle = \text{Re}(\alpha) + i\text{Im}(\alpha)$, and we have used the eigenstates $|m\rangle$ of spin operator J_z and $\alpha(0) = 0$ as the initial states. We plot phase-space trajectories only with $m = 0, \pm 1, \pm 2, \pm 3$ for simple explanation, which clearly show that the coherent wave packet is restored to its original state after a fixed time $t_a = 2\pi/\omega_a$ or integer times of t_a . For different $|m|$, there are different radius circles in the phase-space trajectories, and it is the central symmetry for the opposite m .

The geometric phase, as the enclosed circle area of the trajectory in phase space, is insensitive to the initial phonon state [37], which means $\int_0^{t_a} \alpha(0)e^{-i\omega_a t} = 0$. Thus, the phonon-induced geometry phase is robust against the imperfection of initial phonon state preparation, and we assume $\alpha(0) = 0$ for simplicity. However, the decay and thermal noise of phonons during the spin-phonon interaction will influence the geometry phase accumulation. In this case, the system dynamics follows the master equation

$$\frac{d\rho}{dt} = -i[H, \rho] + \frac{\gamma}{2}(n_{th} + 1)\mathcal{L}(a)\rho + \frac{\gamma}{2}n_{th}\mathcal{L}(a^\dagger)\rho. \quad (2)$$

Here $\gamma = \omega_a/Q$ describes the decay rate of the mechanical mode, n_{th} is the mean phonon number of the mechanical thermal noise, and $\mathcal{L}(o)\rho = 2o\rho o^\dagger - o^\dagger o\rho - \rho o^\dagger o$ is the Lindblad superoperator for given jump operator o . The reduced density matrix of the collective spin can be written as

$$\rho_{\text{spin}} = \sum_{m,n} \rho_{m,n}(0) e^{i\phi_{m,n}(t)} |m\rangle \langle n|. \quad (3)$$

$\phi_{m,n}(t)$ is the phase difference between these spin states. The phase can be solved as

$$\begin{aligned} \phi_{m,n}(t) = & -\left(n_{th} + \frac{1}{2}\right)(n - m)^2 \\ & \times \left\{ \gamma \int_0^t |\alpha(\tau)|^2 d\tau + |\alpha(t)|^2 \right\} \\ & + ig(n^2 - m^2) \text{Re} \int_0^t \alpha(\tau) d\tau. \end{aligned} \quad (4)$$

Here, the amplitude of mechanical resonator is $\alpha(t) = \frac{-ig}{\gamma/2 + i\omega_a} [1 - e^{-(\gamma/2 + i\omega_a)t}]$ [37]. The finite γ of the mechanical resonator introduces decoherence and leads to the first term of the above equation; the second term corresponds to the interaction J_z^2 inducing spin squeezing. Molmer and Sorensen proposed an approach for an ion trap to realize the spin squeezing, which is insensitive to the initial thermal phonon states [38]. Compared to the Molmer-Sorensen scheme in which two-laser pumping and the Lamb-Dicke approximation are required [38], our approach utilizes stable spin-phonon interaction and there is no approximation in our model.

III. SPIN SQUEEZING

The spin squeezing is evaluated by the squeezing parameter [13,16]

$$\xi_N^2 = \frac{\min(\Delta J_{\vec{n}_\perp}^2)}{N/2}, \quad (5)$$

where $\Delta J_{\vec{n}_\perp}^2$ is the variance of spin operators along the direction perpendicular to the mean-spin direction $\vec{n}_0 = \vec{J}/|\langle \vec{J} \rangle|$, which is determined by the expectation values $\langle J_\alpha \rangle$, with $\alpha \in \{x, y, z\}$. For an atomic system initialized in a coherent spin state (CSS) [39] along the x axis, satisfying $J_x |\psi(0)\rangle_{\text{atom}} = N |\psi(0)\rangle_{\text{atom}}$, we have $\rho_{m,n}(0) = 2^{-2N} \sqrt{\frac{(2N)!}{(N-m)!(N+m)!} \frac{(2N)!}{(N-n)!(N+n)!}}$ and $\Delta J_{\vec{n}_\perp}^2 = N/2$. Thus, for squeezed spin states we have $\xi_N^2 < 1$.

First of all, we studied the spin squeezing by Eq. (3) without thermal noise. The squeezing parameters ξ_N^2 as a function of the time (dimensional number gt) for various quality factors Q are plotted in Fig. 2(a). As expected, the effect of the phonon-induced geometry phase leads to the twisting and squeezing of the CSS, thus the ξ_N^2 decreasing with time. After a certain optimal t , the ξ_N^2 increases, due to the overtwisting by the geometry phase, and a high order effect arises. It is shown that the minimal value of the spin-squeezing parameter decreases with higher mechanical quality factor Q . When the quality factor $Q = 1000$ (the black solid line), the almost perfect spin squeezing for the ideal one-axis twisting can be achieved. Including the mechanical thermal noise, squeezing parameters ξ_N^2 as functions of the time with the quality factor $Q = 1000$ are plotted in Fig. 2(b). It is natural that the spin squeezing becomes worse with the increasing of the thermal noise n_{th} . We also studied the suppression of the influence of thermal noise by improving the quality factor Q . As shown in Fig. 2(c), the optimal spin squeezing [the minimum value of the $\xi_N^2(t)$] is plotted against the Q for $n_{th} = 200$, which means that the thermal temperature $T \approx 10$ mK. The ξ_N^2 reduces with Q and

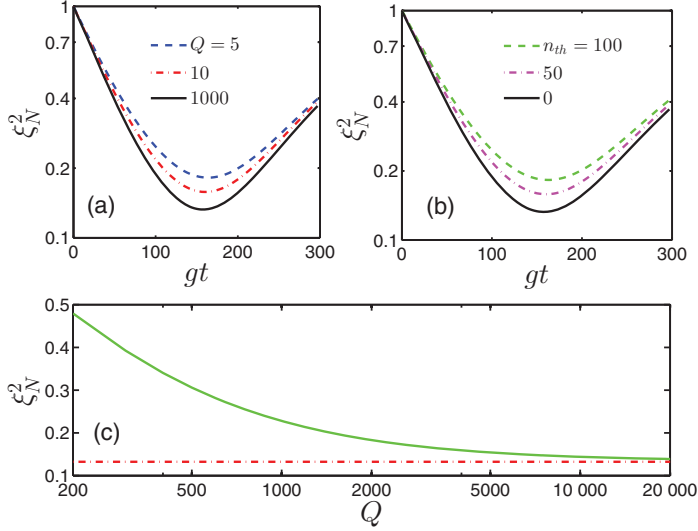


FIG. 2. (Color online) (a) The squeezing parameter ξ_N^2 as a function of the time for $n_{th} = 0$ and various $Q = 5, 10, 1000$ (top to bottom). (b) The squeezing parameter ξ_N^2 as a function of the time for $Q = 1000$ and various $n_{th} = 100, 50, 0$ (top to bottom). (c) The green solid line is optimal squeezing parameter ξ_N^2 versus the quality factor Q for $n_{th} = 200$ ($T \approx 10$ mK), and the red dashed line is the result for ideal one-axis twisting spin squeezing. $N = 10$ for all simulations.

approaches the limit for ideal one-axis twisting spin squeezing (red dashed line).

To understand these results, we simplified the spin-state-dependent geometric phase

$$\phi_{m,n}(t) = \frac{i|g|^2\omega_a t}{(\gamma/2)^2 + \omega_a^2} [(m^2 - n^2) + i\mu(m - n)^2], \quad (6)$$

under the approximation $t \gg \gamma^{-1}$, which means $\alpha(t) = \frac{-ig}{\gamma/2 + i\omega_a}$ and the transient evolution of the mechanical resonator is neglected. Here, the dimensionless factor $\mu = \frac{n_{th} + 1/2}{Q}$. The first term accounts for the coefficient proportional to the time t , and the two terms within the bracket correspond to spin squeezing and decoherence, respectively. Then, we can obtain the degree of spin squeezing for the initial state CSS along the x axis

$$\xi_N^2 = 1 + \frac{2N-1}{4}(A - \sqrt{A^2 + B^2}), \quad (7)$$

where

$$\begin{aligned} A &= 1 - \cos^{2N-2}(2Ct)e^{-4C\mu t}, \\ B &= -4 \sin(Ct) \cos^{2N-2}(Ct)e^{-4C\mu t}. \end{aligned} \quad (8)$$

Here, $Ct = \frac{g}{\omega_a} \frac{1}{1+1/4Q^2} gt$. The analytical solution implies that the spin squeezing is mainly determined by the two dimensionless parameters Ct and μ . For $Q \gg 1$, we have $\frac{1}{1+1/4Q^2} \approx 1$. For $N \gg 1$, we can apply the approximation $\cos^{2N-2}(x) \approx e^{-(N-1)x^2}$ for $x \ll 1$. So, the time required ($gt \approx 160$ in Fig. 2) to achieve the optimal spin squeezing scales with $\frac{1}{\sqrt{N-1}}$. From Eq. (7), we obtain the approximated upper bound of the optimal spin squeezing $\xi_N^2 \lesssim 1 - e^{-\frac{1}{2}-4\frac{\mu}{\sqrt{N}}}/(1 - e^{-1-2\frac{\mu}{\sqrt{N}}})$, which indicates that the ratio $\frac{\mu}{\sqrt{N}} = \frac{n_{th} + 1/2}{Q\sqrt{N}}$ should be as small as possible. As long as $\frac{n_{th} + 1/2}{Q\sqrt{N}} < 10^{-3}$, we can achieve

squeezing almost as good as the best squeezing achievable with ideal single axes twisting [Fig. 2(c)].

IV. BANG-BANG CONTROL

During the preparation of optimal SSS, there are inevitable couplings between the system and baths. For example, the lattice vibrations and environment spins will induce dephasing and destroy the spin squeezing. The dynamical decoupling technique is well known for protecting coherence from environment [40–47], and now we apply the bang-bang (BB) pulses [40] to suppress the decoherence. The sequence consists of M pulses, which split the total time interval t into M small intervals $t_p = \frac{p}{M}t$ with $p = 1, 2, \dots, M$. The pulses rotate the collective spin states around the y axis, and we chose the pulse sequence to rotate π and $-\pi$ alternately, which leads to $e^{i\pi J_y} \sigma_{zj} e^{-i\pi J_y} = -\sigma_{zj}$ and $e^{i\pi J_y} J_z^2 e^{-i\pi J_y} = J_z^2$. Therefore, the spin squeezing J_z^2 is conserved while the σ_z is inverted by the BB pulses. Considering the $2N$ qubits which are independently coupled to thermal baths, the Hamiltonian from Eq. (1) is changed to

$$\begin{aligned} H' &= \omega_a a^\dagger a + g\varepsilon(t)J_z(a + a^\dagger) + \sum_k \omega_k b_k^\dagger b_k \\ &+ \sum_{j=1}^{2N} \sum_k \frac{\varepsilon(t)\sigma_{zj}}{2} h_{kj}(b_k + b_k^\dagger). \end{aligned} \quad (9)$$

Here, b_k and b_k^\dagger are the creation and annihilation bosonic operators of the k th bath mode, which couples to the j th spin with coupling strength h_{kj} . The switch function $\varepsilon(\tau)$ due to BB pulses is given by $\varepsilon(\tau) = \sum_{p=1}^M (-1)^p \theta(\tau - t_p) \theta(t_{p+1} - \tau)$ with $\theta(t)$ the Heaviside step function.

With the decoherence and BB, the geometry phase factor [Eq. (4)] of spin states is solved as

$$\begin{aligned} \phi'_{m,n}(t) &= -\left(n_{th} + \frac{1}{2}\right)(n - m)^2 \\ &\times \left\{ \gamma \int_0^t |\alpha'(\tau)|^2 d\tau + |\alpha'(t)|^2 \right\} \\ &+ ig(n^2 - m^2) \text{Re} \int_0^t \varepsilon(\tau) \alpha'(\tau) d\tau - \kappa_{m,n}(t). \end{aligned} \quad (10)$$

Here, $\alpha'(t) = -ig \int_0^t \varepsilon(\tau) e^{-(\frac{\gamma}{2} + i\omega_a)(t-\tau)} d\tau$ and $\kappa_{m,n}(t)$ is due to the decoherence. Assuming that the baths to each spin are Ohmic [48] and have the same spectral density $\eta\omega e^{-\frac{\omega}{\omega_c}}$, we have

$$\kappa_{m,n}(t) \leq (|n - m| + 2) \int_0^\infty G(\omega) F_M(\omega, t) d\omega, \quad (11)$$

where the modulation spectrum is $F_M(\omega, t) = \frac{\tan^2(\frac{\omega t}{2M+2}) [1 + (-1)^M \cos(\omega t)]}{\omega^2}$, the temperature-dependent interacting spectrum is $G(\omega) = \eta\omega e^{-\frac{\omega}{\omega_c}} (\frac{2}{e^{2\lambda\omega} - 1} + 1)$ [46], in which η is the coupling strength between the system and the bath modes, ω_c is the cutoff frequency, and $\lambda = 1/\kappa_B T_b$ is the inverse temperature. This time-dependent dephasing is a non-Markovian process [49], which is a constant under the Markovian approximation [26]. In order to simplify the calculation, we use the upper limit instead of the $\kappa_{m,n}(t)$.

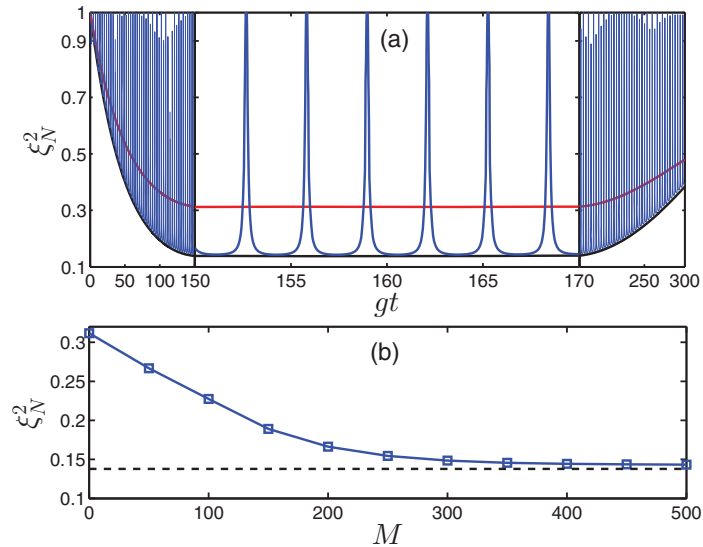


FIG. 3. (Color online) (a) The squeezing parameter ξ_N^2 as a function of the time gt . The parameters are $\eta = 0, M = 0$ (black line), $\eta = 4 \times 10^{-4}, M = 0$ (red line), and $\eta = 4 \times 10^{-4}, M = 500$ (blue line). (b) The blue solid line for the optimal squeezing parameter ξ_N^2 versus the pulses M for $\eta = 4 \times 10^{-4}$, and the black dashed line for the result without thermal baths. Other parameters are $n_{th} = 200$ ($T \approx 10$ mK), $\omega_c = g, \lambda = 4/g, Q = 20000$, and $N = 10$.

In Fig. 3(a), we numerically calculated squeezing parameter ξ_N^2 as a function of time for various η and M . Since the decoherence term $\kappa_{m,n}(t)$ is proportional to the coupling strength between the system and the bath modes, we observe the increment of the optimal ξ_N^2 for increasing η (black and red lines). The blue line shows the suppression of decoherence by BB, and here we choose the sequence number $M = 500$ and $\eta = 4 \times 10^{-4}$, which is in contrast to the red line. There are periodic peaks with the separation distance $\Delta gt = \pi$, and the peak values are obtained when $gt = (n + 1/2)\pi$; n is integer. This phenomena can be interpreted as follows: the BB pulse period is $t_M = t/M$, and the time period for the phonon state trajectories in the phase space (Fig. 1) is $t_a = 2\pi/\omega_a$. For $M = 500$ and $\omega_a/g = 1000$, we have $t_M/t_a = gt/\pi$. When $gt/\pi = n$ is integer, the geometric phase is always cumulative, and the coherent spin squeezing effect is not degraded by the BB pulse sequence. In contrast, when $gt/\pi = n + \frac{1}{2}$, the geometric phase imprints alternating sign as function of M , and then the spin squeezing is weakened. Comparing the minima of ξ_N^2 with BB (blue line) to the results without BB (black and red lines), the undesired effect of decoherence is effectively suppressed by the dynamical decoupling. Figure 3(c) shows the optimal ξ_N^2 versus the pulse sequence length M . With increasing M , the optimal value of ξ_N^2 is improved and

approaches the black dashed line, which is the ideal result determined by Eq (6) without thermal baths. When $M \geq 400$, the influence of thermal baths on spin squeezing can be almost eliminated, which means $\kappa_{m,n}(t) \approx 0$.

V. EXPERIMENTAL REALIZATION

The possible experimental configurations are a diamond nanostring oscillator and diamond nanocrystal adhering to a cantilever. For the first approach, the diamond nanostring with nanoscale cross section can be fabricated with the approaches in Ref. [32], with frequency above 1 MHz and quality factor as large as 10^5 . For the second approach, a diamond nanocrystal can be attached to a cantilever [7,28] and close to a nanomagnet, the cantilever frequency around 1 MHz and quality factor exceeding 10^4 . For both approaches, NV^- centers can be generated by ion implantation in diamond nanocrystal or at selected location of the diamond nanostring. A reasonable density can be about 100 ppm, leading to the spin ensemble of $N \sim 20$ in a $10 \times 10 \times 10$ nm³ volume of diamond. As the spin squeezing depends on the dimensionless parameter $T/Q\sqrt{N}$, we can relax the requirement for low temperature by increasing the mechanical Q or the ensemble size.

VI. CONCLUSION

An approach to achieve spin squeezing by phonon-induced geometric phase is proposed. This scheme is feasible for experiments on a solid state spin ensemble coupled to a mechanical oscillator. With reasonable parameters, the ultimate limit of the ideal one-axis twisting spin squeezing can be achieved as long as the quality factor is sufficiently high that $Q > \frac{n_{th}+1/2}{\sqrt{N}} \times 10^3$. The decoherence due to spin-bath coupling can be effectively suppressed by the bang-bang pulses. This geometric-phase-based spin squeezing can be used to significantly improve the sensitivity of magnetic sensing with nitrogen-vacancy spin ensembles. Moreover, the technique can be generalized to spin ensembles coupled to other high- Q bosonic modes that prepare quantum states by geometry phase.

ACKNOWLEDGMENTS

We thank Peter Rabl for useful suggestions. This work was supported by the National Basic Research Program of China (Grant No. 2011CBA00200, and National Natural Science Foundation of China (Grants No. 11274295 and No. 11474271). L.J. acknowledges support from the Alfred P. Sloan Foundation, the Packard Foundation, the AFOSR-MURI (USA), the ARO (USA), and the DARPA Quiness (USA) program.

- [1] L. Childress and R. Hanson, *MRS Bull.* **38**, 134 (2013).
 [2] L. Rondin, J.-P. Tetienne, T. Hingant, J.-F. Roch, P. Maletinsky, and V. Jacques, *Rep. Prog. Phys.* **77**, 056503 (2014).
 [3] G. Balasubramanian *et al.*, *Nat. Mater.* **8**, 383 (2009).

- [4] F. Jelezko, T. Gaebel, I. Popa, M. Domhan, A. Gruber, and J. Wrachtrup, *Phys. Rev. Lett.* **93**, 130501 (2004).
 [5] L. Childress, M. V. G. Dutt, J. M. Taylor, A. S. Zibrov, F. Jelezko, J. Wrachtrup, P. R. Hemmer, and M. D. Lukin, *Science* **314**, 281 (2006).

- [6] P. Ouartchaiyapong, K. W. Lee, B. A. Myers, and A. C. B. Jayich, *Nat. Commun.* **5**, 4429 (2014).
- [7] S. Kolkowitz, A. C. B. Jayich, Q. P. Unterreithmeier, S. D. Bennett, P. Rabl, J. G. E. Harris, and M. D. Lukin, *Science* **335**, 1603 (2012).
- [8] J. R. Maze *et al.*, *Nature (London)* **455**, 644 (2008).
- [9] L. M. Pham *et al.*, *New J. Phys.* **13**, 045021 (2011).
- [10] G. Kucsko, P. C. Maurer, N. Y. Yao, M. Kubo, H. J. Noh, P. K. Lo, H. Park, and M. D. Lukin, *Nature (London)* **500**, 54 (2013).
- [11] F. Dolde, H. Fedder, M. W. Doherty, T. Nöbauer, F. Rempp, G. Balasubramanian, T. Wolf, F. Reinhard, L. C. L. Hollenberg, F. Jelezko, and J. Wrachtrup, *Nat. Phys.* **7**, 459 (2011).
- [12] V. Giovannetti, S. Lloyd, and L. Maccone, *Nat. Photonics* **5**, 222 (2011).
- [13] M. Kitagawa and M. Ueda, *Phys. Rev. A* **47**, 5138 (1993).
- [14] W. M. Itano, J. C. Bergquist, J. J. Bollinger, J. M. Gilligan, D. J. Heinzen, F. L. Moore, M. G. Raizen, and D. J. Wineland, *Phys. Rev. A* **47**, 3554 (1993).
- [15] D. J. Wineland, J. J. Bollinger, W. M. Itano, and D. J. Heinzen, *Phys. Rev. A* **50**, 67 (1994).
- [16] J. Ma, X. G. Wang, C. P. Sun, and F. Nori, *Phys. Rep.* **509**, 89 (2011).
- [17] M. F. Riedel, P. Böhi, Y. Li, T. W. Hänsch, A. Sinatra, and P. Treutlein, *Nature (London)* **464**, 1170 (2010).
- [18] S. Chaudhury, S. Merkel, T. Herr, A. Silberfarb, I. H. Deutsch, and P. S. Jessen, *Phys. Rev. Lett.* **99**, 163002 (2007).
- [19] R. Inoue, S.-I.-R. Tanaka, R. Namiki, T. Sagawa, and Y. Takahashi, *Phys. Rev. Lett.* **110**, 163602 (2013).
- [20] M. Ueda, T. Wakabayashi, and M. Kuwata-Gonokami, *Phys. Rev. Lett.* **76**, 2045 (1996).
- [21] M. Takeuchi, S. Ichihara, T. Takano, M. Kumakura, T. Yabuzaki, and Y. Takahashi, *Phys. Rev. Lett.* **94**, 023003 (2005).
- [22] M. H. Schleier-Smith, I. D. Leroux, and V. Vuletić, *Phys. Rev. A* **81**, 021804 (2010).
- [23] I. D. Leroux, M. H. Schleier-Smith, and V. Vuletić, *Phys. Rev. Lett.* **104**, 073602 (2010).
- [24] E. G. Dalla Torre, J. Otterbach, E. Demler, V. Vuletic, and M. D. Lukin, *Phys. Rev. Lett.* **110**, 120402 (2013).
- [25] Y.-L. Zhang, C.-L. Zou, X.-B. Zou, L. Jiang, and G.-C. Guo, *Phys. Rev. A* **91**, 033625 (2015).
- [26] S. D. Bennett, N. Y. Yao, J. Otterbach, P. Zoller, P. Rabl, and M. D. Lukin, *Phys. Rev. Lett.* **110**, 156402 (2013).
- [27] K. Fang, V. M. Acosta, C. Santori, Z. Huang, K. M. Itoh, H. Watanabe, S. Shikata, and R. G. Beausoleil, *Phys. Rev. Lett.* **110**, 130802 (2013).
- [28] D. Rugar, R. Budakian, H. J. Mamin, and B. W. Chui, *Nature (London)* **430**, 329 (2004).
- [29] J. Teissier, A. Barfuss, P. Appel, E. Neu, and P. Maletinsky, *Phys. Rev. Lett.* **113**, 020503 (2014).
- [30] M. Ganzhorn, S. Klyatskaya, M. Ruben, and W. Wernsdorfer, *Nat. Nanotechnol.* **8**, 165 (2013).
- [31] Y. Tian, P. Navarro, and M. Orrit, *Phys. Rev. Lett.* **113**, 135505 (2014).
- [32] M. J. Burek, D. Ramos, P. Patel, I. W. Frank, and M. Lončar, *Appl. Phys. Lett.* **103**, 131904 (2013).
- [33] M. K. Zalalutdinov, M. P. Ray, D. M. Photiadis, J. T. Robinson, J. W. Baldwin, J. E. Butler, T. I. Feygelson, B. B. Pate, and B. H. Houston, *Nano Lett.* **11**, 4304 (2011).
- [34] Y. Tao, J. M. Boss, B. A. Moores, and C. L. Degen, *Nat. Commun.* **5**, 3638 (2014).
- [35] P. Rabl, P. Cappellaro, M. V. Gurudev Dutt, L. Jiang, J. R. Maze, and M. D. Lukin, *Phys. Rev. B* **79**, 041302(R) (2009).
- [36] S. Puri, N. Y. Kim, and Y. Yamamoto, *Phys. Rev. B* **85**, 241403(R) (2012).
- [37] J. J. García-Ripoll, P. Zoller, and J. I. Cirac, *Phys. Rev. A* **71**, 062309 (2005).
- [38] K. Mølmer and A. Sørensen, *Phys. Rev. Lett.* **82**, 1835 (1999).
- [39] F. T. Arecchi, E. Courtens, R. Gilmore, and H. Thomas, *Phys. Rev. A* **6**, 2211 (1972).
- [40] L. Viola and S. Lloyd, *Phys. Rev. A* **58**, 2733 (1998).
- [41] L.-A. Wu and D. A. Lidar, *Phys. Rev. Lett.* **88**, 207902 (2002).
- [42] J. Du, X. Rong, N. Zhao, Y. Wang, J. Yang, and R. B. Liu, *Nature (London)* **461**, 1265 (2009).
- [43] G. de Lange, Z. H. Wang, D. Ristè V. V. Dobrovitski, and R. Hanson, *Science* **330**, 60 (2010).
- [44] L. Jiang and A. Imambekov, *Phys. Rev. A* **84**, 060302 (2011).
- [45] W. Yang, Z.-Y. Wang, and R.-B. Liu, *Front. Phys. China* **6**, 2 (2011).
- [46] Q. S. Tan, Y. X. Huang, L. M. Kuang, and X. G. Wang, *Phys. Rev. A* **89**, 063604 (2014).
- [47] N. Zhao and Z. Q. Yin, *Phys. Rev. A* **90**, 042118 (2014).
- [48] A. J. Leggett, S. Chakravarty, A. T. Dorsey, Matthew P. A. Fisher, Anupam Garg, and W. Zwerger, *Rev. Mod. Phys.* **59**, 1 (1987).
- [49] P. Haikka, T. H. Johnson, and S. Maniscalco, *Phys. Rev. A* **87**, 010103(R) (2013).